Organic & Biomolecular Chemistry

Dynamic Article Links

Cite this: *Org. Biomol. Chem.*, 2011, **9**, 3681

www.rsc.org/obc

PAPER

Anti-virulence Strategy against *Brucella suis*: Synthesis, Biological Evaluation and Molecular Modeling of Selective Histidinol Dehydrogenase Inhibitors

Marie-Rose Abdo,[a] Pascale Joseph,[b] Jérémie Mortier,[c] François Turtaut,[a] Jean-Louis Montero,[a] Bernard Masereel,[c] Stephan Köhler*[b] and Jean-Yves Winum*[a]

Received 27th January 2011, Accepted 7th March 2011
DOI: 10.1039/c1ob05149k

In the facultative intracellular pathogen *Brucella suis*, histidinol dehydrogenase (HDH) activity, catalyzing the last step in histidine biosynthesis, is essential for intramacrophagic replication. The inhibition of this virulence factor by substituted benzylic ketones was a proof of concept that disarming bacteria leads to inhibition of intracellular bacterial growth in macrophage infection. This work describes the design, synthesis and evaluation of 19 new potential HDH inhibitors, using a combination of classical approaches and docking studies. The IC_{50}-values of these inhibitors on HDH activity were in the nanomolar range, and several of them showed a 70–100% inhibition of *Brucella* growth in minimal medium. One selected compound yielded a strong inhibitory effect on intracellular replication of *B. suis* in human macrophages at concentrations as low as 5 μM, with an overall survival of intramacrophagic bacteria reduced by a factor 10^3. Docking studies with two inhibitors showed a good fitting in the catalytic pocket and also interaction with the second lipophilic pocket binding the cofactor NAD^+. Experimental data confirmed competition between inhibitors and NAD^+ at this site. Hence, these inhibitors can be considered as promising tools in the development of novel anti-virulence drugs.

Introduction

Bacterial infections represent a serious public health problem worldwide. The widespread emergence of resistance and multi-resistance to antibiotics among a growing number of bacterial pathogens represents a major threat and necessitates the development of new molecules with innovative mechanisms of action.[1] In the past few years, the growing information on the virulence mechanisms of various pathogens in the relationship with their hosts led to increased interest in the potential definition of virulence factors as novel targets for anti-infectious agents.[2]

In intracellular bacteria such as *Brucella* spp., virulence is linked to the capacity of the pathogen to replicate inside the macrophage host cell and to escape from the host immune system.[3]

Brucella spp. are the etiological agents of brucellosis, the major bacterial zoonosis worldwide. They are facultative intracellular coccobacilli, pathogenic for a variety of mammals including ruminants and humans. Human brucellosis may become chronic, eventually causing death. Treatment of human brucellosis may last for several months and cases of relapse may be observed, reducing the efficacy of the therapy. Moreover, there is no human vaccine against brucellosis.[4]

The genes required for intramacrophagic replication of *Brucella* are a subset of the virulence genes of the pathogen and have been called the intramacrophagic virulome.[3] Definition of the targets for antibacterials by analysis of the intramacrophagic virulome should limit the selective pressure to the intracellular niche and also reduce the probability of affecting the commensal flora. Among those virulence genes, we identified, cloned and overexpressed *hisD* (BR0252) from *Brucella suis*, which encodes the histidinol dehydrogenase (HDH; EC 1.1.1.23), and we purified this metalloenzyme which catalyses the final steps in the histidine biosynthetic pathway (Fig. 1).[5,6] The essential character of histidine biosynthesis for virulence has been demonstrated in other pathogenic bacteria such as *Salmonella typhimurium*, *Burkholderia pseudomallei* and *Mycobacterium tuberculosis*.[7] First series of HDH inhibitors, being substituted benzylic ketones, were designed

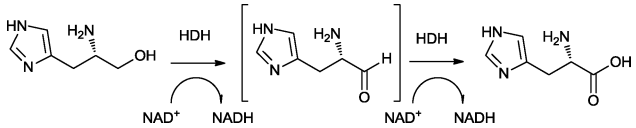

Fig. 1 Histidine biosynthesis steps catalyzed by histidinol dehydrogenase HDH.

[a]*Institut des Biomolécules Max Mousseron (IBMM), UMR 5247 CNRS-Université Montpellier I-Université Montpellier II, Ecole Nationale Supérieure de Chimie de Montpellier, 8 rue de l'Ecole Normale, 34296, Montpellier Cedex, France. E-mail: jean-yves.winum@univ-montp2.fr; Tel: +33-467147234*

[b]*Centre d'études d'agents Pathogènes et Biotechnologie pour la Santé (CPBS), UMR 5236 CNRS-Université Montpellier I-Université Montpellier II, 1919 Route de Mende, 34293, Montpellier Cedex 5, France. E-mail: Stephan.Kohler@cpbs.cnrs.fr*

[c]*Drug Design & Discovery Center, Department of Pharmacy, University of Namur (FUNDP), Belgium*

and synthesized by this group, and their potential inhibitory effect on purified *Brucella* HDH was studied.[5,6]

The synthetic products most active on the purified enzyme exhibited IC_{50} inhibition activities in the nanomolar range. These novel inhibitors against a virulence factor were a proof of concept that disarming bacteria leads to the inhibition of intracellular bacterial growth in experimental macrophage infection experiments[5,6] Therefore, HDH represents a selective and promising target for the development of new antibacterial agents, favouring the development of HDH inhibitors.

These encouraging findings resulted in the design and synthesis of additional structures, by developing new HDH inhibitors using a combination of classical approaches and docking studies. Starting from our first lead inhibitor and using palladium-catalyzed reactions, we developed a library of inhibitors aiming at an increased potency within the benzylic ketone series. (Fig. 2).

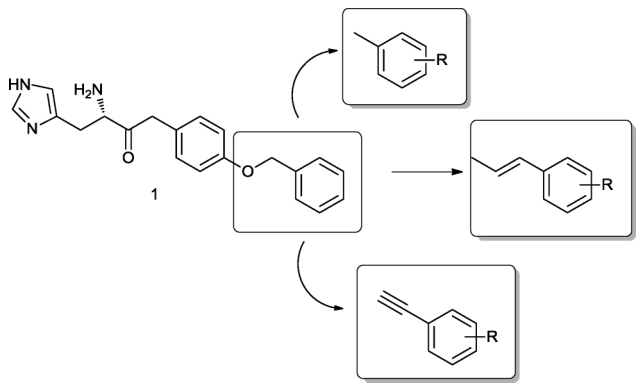

Fig. 2 Design of improved HDH inhibitors by optimization of the initial hit compound **1**.

Results and discussion

Chemistry

Encouraged by the promising HDH inhibitory activity of **1** (IC_{50} = 3nM), we started a systematic structure modification program to increase the potency and to understand the structural requirements for the key side chain by optimizing the interactions with the enzyme active site. To this end, three structural types of side chains, comprising *para*-substitution patterns in phenyl rings were synthesized.

We envisioned that the synthetically easiest and most flexible approach for the introduction of the different chains would be based on the use of palladium-catalyzed reactions such as Suzuki and Sonogashira reactions. Preparation of the different compounds was achieved in a two-step-synthesis starting from the fully protected L-histidine methyl ester **2**, previously described by our group.[6] By reacting the corresponding aryl or vinyl or alkyl boronic acid under Suzuki reaction conditions, followed by a acidic total deprotection of the resulting compounds, we obtained the series of inhibitors **3–6**, as outlined in Scheme 1.

Further elaboration of new inhibitors was also accomplished starting from the key derivative **2**, by applying a Sonogashira strategy with different substituted alkynes. In this case, experimental conditions were optimized and the best results were obtained using a palladium catalyst and copper co-catalyst at 10 mol% in THF in the presence of triethylamine as base. Final hydrolysis under acidic conditions yielded the series of compounds **7** (Scheme 2).

Biological Evaluation

Enzymatic assays: HDH inhibition study. The series of compounds **3–7** were tested for their inhibitory activity against purified

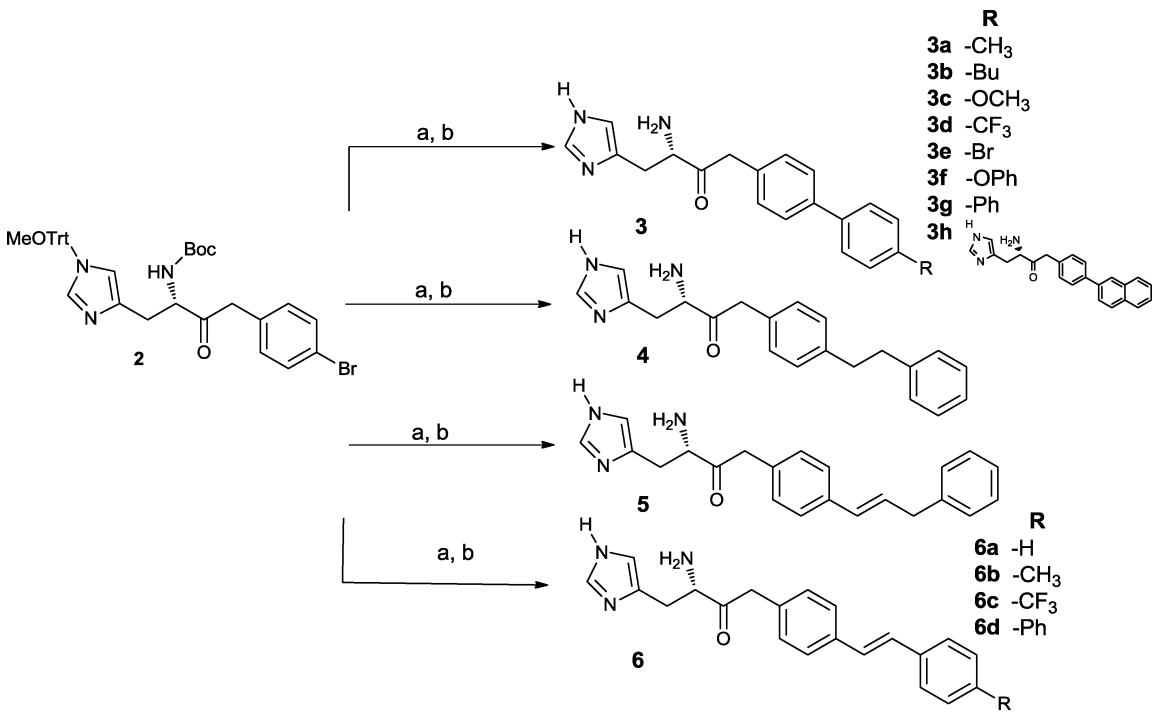

Scheme 1 Synthesis of HDH inhibitors **3–6** *via* Suzuki coupling. Reagents and conditions: (a) R-$B(OH)_2$, $Pd(Ph_3)_4$, Na_2CO_3, Toluene; (b) HCl 4 M, dioxane.

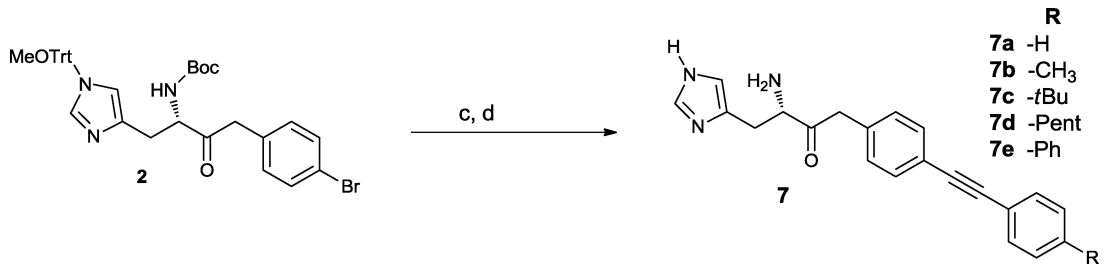

Scheme 2 Synthesis of HDH inhibitors **7** *via* Sonogashira coupling. Reagents and conditions: (a) Arylalkyne, $Pd(Ph_3)_4$, NEt_3, CuI, PPh_3, THF; (b) HCl 4 M, dioxane.

Table 1 Inhibition of *B. suis* histidinol dehydrogenase with compounds **3–7**. The values are means of three independent assays. Variations were in the range of 5–10% of the shown data. Nd: not determined

Compounds	IC_{50} (nM) on HDH (*B. suis*)
1	3
3a	30
3b	40
3c	20
3d	30
3e	nd
3f	70
3g	nd
3h	30
4	13
5	30
6a	25
6b	40
6c	65
6d	nd
7a	3
7b	40
7c	65
7d	8.5
7e	nd

B. suis HDH protein (see experimental section). Inhibition data are presented in Table 1. All compounds **3–7** were nanomolar inhibitors with $IC_{50} \leq 70$ nM. Most of the biphenyl compounds (**3a–3h**) showed an inhibitory potency in the range of 20–70nM, demonstrating the poor influence of the nature of R.

Compounds containing phenyl alkynyl moiety such as **7a** and **7d** displayed the most potent activity with an IC_{50} of 3 and 8.5 nM, respectively. Potent inhibition was also observed for compounds **4**, **5** and **6**, with IC_{50} concentrations ranging from 13 to 70 nM. Collectively, these results demonstrate that subtle structural differences in the tail of the molecules can influence enzyme inhibition characteristics.

Inhibition of growth of *B. suis* in minimal medium. Following the determination of the IC_{50} values for various molecules, the effect of selected HDH inhibitors on growth of *B. suis* in minimal medium, requiring histidine biosynthesis, was studied. After incubation at 37 °C with shaking and aeration for 7 days, molecules **3d**, **3f**, and especially **3h**, **6b**, and **7a** showed a 70–100% inhibition of *Brucella* growth, as compared to an untreated control culture (Table 2). To obtain satisfactory inhibition rates, concentration of approximately 50 μM were necessary, which is roughly 1000-fold higher than the IC_{50} described above. The most likely explanation for this observation is the existence of a physical barrier, represented by the outer and inner membranes

Table 2 % Inhibition of *B. suis* growth *in vitro* in minimal medium in the presence of various selected inhibitors at final concentrations of 100 μM or 50 μM, measured at 7 days post inoculation. The growth curve obtained in untreated medium was used as reference

	% Inhibition of *B. suis* growth in minimal medium by HDH inhibitors at a concentration of	
Compounds	100 μM	50 μM
3a	40	30
3b	60	50
3c	60	30
3d	90	70
3f	90	70
3h	100	100
6b	100	100
7a	100	100
7c	30	30
7d	30	30

of the bacterium. Inhibitors have to cross the membranes by passive diffusion, whereas in the enzymatic assays, purified HDH was in direct contact with the molecules. The observed growth inhibition of live brucellae is a specific effect on HDH, as we have previously published that competitive addition of histidine relieves the inhibition.[6b]

Inhibition of intramacrophagic replication of *B. suis*. Compound **7a**, the molecule with the lowest IC_{50} among the molecules tested (Table 1) and with a 100%-inhibition of *Brucella* growth in minimal medium (Table 2), was selected to test the potential effects of this HDH-inhibitor on intracellular replication of *B. suis* in human macrophages. As shown in Fig. 3, the compound had a strong inhibitory effect on intracellular growth of *Brucella* at concentrations as low as 5 μM. The overall survival of intramacrophagic bacteria was reduced by a factor 10^3 over the infection period of 24 h. The viability of the macrophages was not affected under these conditions, as determined by using trypan blue coloration (not shown).

These results clearly show that the HDH inhibitor reaches the target enzyme located in the bacterial cytoplasm, following diffusion across both eukaryotic and bacterial membranes, hence affecting histidine biosynthesis which is essential for the growth of *Brucella* at the intracellular state.

Molecular modeling and docking study

No experimentally-derived structural data for the *B. suis* isoform of HDH have been reported to date allowing to study the molecules within the 3-D structure of the target enzyme. Following a

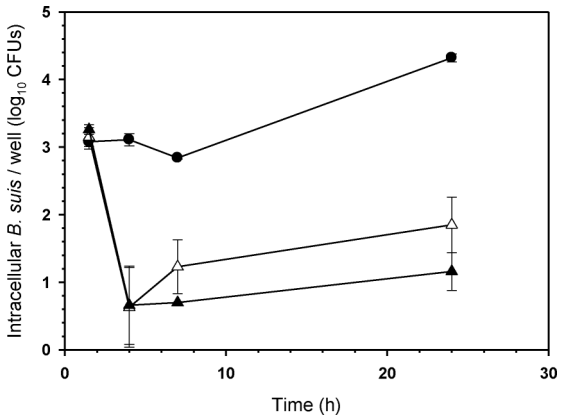

Fig. 3 Intramacrophagic survival of *B. suis* in untreated human macrophage-like THP-1 cells (●), or in cells treated with 5 μM (△) or 10 μM (▲) of compound **7a**.

BLASTP alignment,[8] *E. coli* HDH was identified as having the protein sequence most similar to *B. suis* HDH, sharing 41% sequence identity and up to 57% sequence homology (similar residues). As the *E. coli* HDH has been cocristallized with NAD+ and histidine, and its structure solved (PDB code 1KAE),[9] the reliability of a docking study of *B. suis* HDH inhibitors within its *E. coli* isoform was considered.

The 40 *E. coli* HDH residues whose side chain are located in a 6 Å-volume around the co-crystallized ligands (NAD^+ and histidine) were selected, and their positions in the alignment to the *B. suis* HDH were analyzed (Fig. 4). An extremely high identity between both cavities was highlighted, since 37 out of 40 residues were perfectly recovered, including key residues in complex with the Zn^{2+} cation (Q259, H262, D360 and H419) and residues H-bonding the histidine scaffold in the catalytic pocket (S237, H327, E356, D360 and E414). In the sequences alignment, two *E. coli* residues (T141 and F213) were identified as different but similar to those of *B.suis* (S141 and Y216). Nevertheless, as T141 is H-bonding the nitrogen atom of the amide function in the NAD^+ structure, this interaction is perfectly conserved with the substituted serine in the *B. suis* HDH sequence. A Π–Π stacking is also observed between the aromatic side chain of F213 and the adenine moiety of the cofactor.

No major change is then observed in the environment of NAD^+ when the phenylalanine is switched to a tryptophan, as reported in the alignment (Fig. 4). Finally, only one residue emerged as really different in this alignment: a leucine (L138) in *E. coli* which was substituted by a tryptophan (Y128) in *B. suis*. This amino acid is located between the histidine/Zn^{2+} cavity and the NAD^+ pocket in the 3D-structure.

Once this very high similarity between both enzymatic cavities demonstrated, *E. coli* HDH can be considered as a very reliable 3D-model to investigate, by molecular modeling, the histidine derivatives series as *B. suis* HDH inhibitors.

Structures **1** and **7a** were then docked inside the enzymatic cavity of HDH using the automated *GOLD* program.[10] For each

```
E.Coli  15   EQQRQLLMRPAISASESITRTVNDILDNVKARGDEALREYSAKFDKTTV--TALKVSAEE  72
             EQ+    +      SE + R V +I+D V+  GD AL +YS +FD+  +  T + V+  E
Br.Suis 13   EQKFAAFLSGKREVSEDVDRAVREIVDRVRREGDSALLDYSRRFDRIDLEKTGIAVTEAE  72

E.Coli  73   IAAASERLSDELKQAMAVAVKNIETFHTAQKLPPVDVETQP-GVRCQQVTRPVASVGLYI  131
             I AA +       +A+ +A   IE  H A++LP  D  T   GV        + +VGLY+
Br.Suis 73   IDAAFDAAPASTVEALKLARDRIEKHH-ARQLPKDDRYTDALGVELGSRWTAIEAVGLYV  131

E.Coli  132  PGGSAPLFSTVLMLATPASIAGCKKVVLCSPPPIADE---ILYAAQLCGVQDVFNVGGAQ  188
             PGG+A   S+VLM A PA +AG  ++V+  P P  +    +L AA+L GV +++ VGGAQ
Br.Suis 132  PGGTASYPSSVLMNAMPAKVAGVDRIVMVVPAPDGNLNPLVLVAARLAGVSEIYRVGGAQ  191

E.Coli  189  AIAALAFGTESVPKVDKIFGPGNAFVTEAKRQVSQRLDGAAIDMPAGPSEVLVIADSGAT  248
             AIAALA+GTE++  V KI GPGNA+V  AKR V        IDM AGPSEVL++AD
Br.Suis 192  AIAALAYGTETIRPVAKIVGPGNAYVAAAKRIV---FGTVGIDMIAGPSEVLIVADKDNN  248

E.Coli  249  PDFVASDLLSQAEHGPDSQVILLTPAADMARRVAEAVERQLAELPRAETARQAL-NASRL  307
             PD++A+DLL+QAEH   +Q IL+T     A  V EAVERQL  L R ETA  +  +   +
Br.Suis 249  PDWIAADLLAQAEHDTAAQSILMTNDEAFAHAVEEAVERQLHTLARTETASASWRDFGAV  308

E.Coli  308  IVTKDLAQCVEISNQYGPEHLIIQTRNARELVDSITSAGSVFLGDWSPESAGDYASGTNH  367
             I+ KD    + ++N+   EHL I   +A   V  I +AGS+F+G ++PE  GDY  G NH
Br.Suis 309  ILVKDFEDAIPLANRIAAEHLEIAVADAEAFVPRIRNAGSIFIGGYTPEVIGDYVGGCNH  368

E.Coli  368  VLPTYGYTATCSSLGLADFQKRMTVQELSKEGFSALASTIETLAAAERLTAHKNAVTLRV  427
             VLPT       S L + D+ KR ++ +L  E   AL      +A AE L AH  +V +R+
Br.Suis 369  VLPTARSARFSSGLSVLDYMKRTSLLKLGSEQLRALGPAAIEIARAEGLDAHAQSVAIRL  428

E.Coli  428  N  428
             N
Br.Suis 429  N  429
```

Fig. 4 Swissprot (BLASTP)[8] alignment of the HDH sequences from *E. coli* and *B. suis*, performed using a compositional matrix adjustment method. Identities = 174/421 (41%), Positives = 242/421 (57%), Gaps = 11/421 (2%). Residues from the enzymatic pocket are highlighted in green (perfect alignment), magenta (favourable alignment) and red (unfavourable alignment).

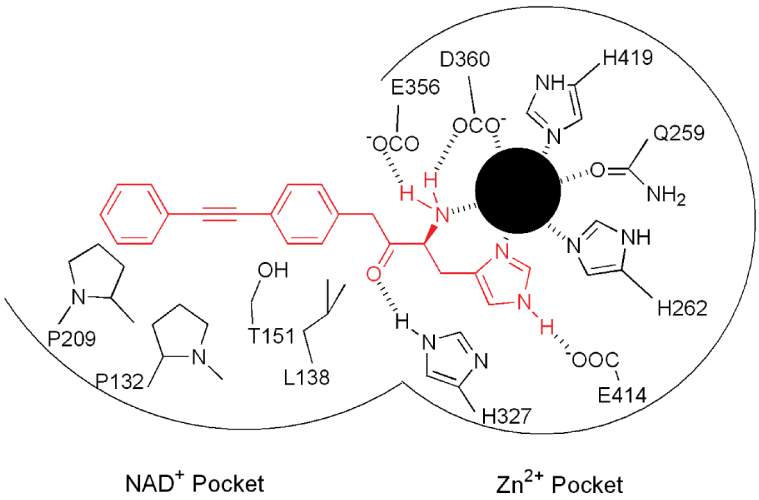

Scheme 3 2D-representation of the binding mode of inhibitor **7a**.

molecule, 20 conformations were generated and the conformation with the best GOLDSCORE was further evaluated as the most probable docking orientation. As a result, each molecule fits very well in the catalytic pocket adopting a similar binding orientation to histidine, the co-crystallized ligand, and product of HDH. As expected, the zinc cation is coordinated with four nitrogen atoms belonging to three imidazole moieties (H262, H419, compound **7a**), and with the amino group of **7a** (Scheme 3). Two nitrogen lone pairs are predicted to be very available thanks to a particular environment where the imidazole NH hydrogen is attracted by the negatively charged E414 side chain and the amino NH_2 hydrogen's are involved in H-bonds with D360, E356 and S237 side chains. This Zn^{2+} pocket is therefore targeted by each synthesized compound, stabilized by the same key interactions as observed for histidine.

Interestingly, the aromatic side-chain is oriented directly towards the NAD^+ pocket, predicting a competition between this type of inhibitors and the cofactor (Fig. 5). This region is hydrophobic and open to the solvent, predicting a good affinity for this lipophilic part of the molecules. Surprisingly, the aromatic side-chains of both nanomolar inhibitors **1** and **7a** are oriented in the same direction in the NAD^+ pocket. A superimposition of **7a** and NAD^+ structures allowed the demonstration that an identical volume was occupied in the active site (Fig. 6). This result is indicative of a pharmacophore structure interacting most favorably with this region and where two axial and almost perpendicular aromatic planes are separated by 3.60 Å to 4.10 Å. Finally, after a validation of the closest structural data available and despite potential subtle structural effects beyond the residue changes between *Brucella* and *E. coli* HDH, the inhibition properties of this chemical series against our target was rationalized. This molecular modeling study demonstrated the high capacity of both compounds to complex the cation Zn^{2+} in the hydrophilic histidine pocket, and to reach the second lipophilic pocket where the NAD^+ cofactor binds.

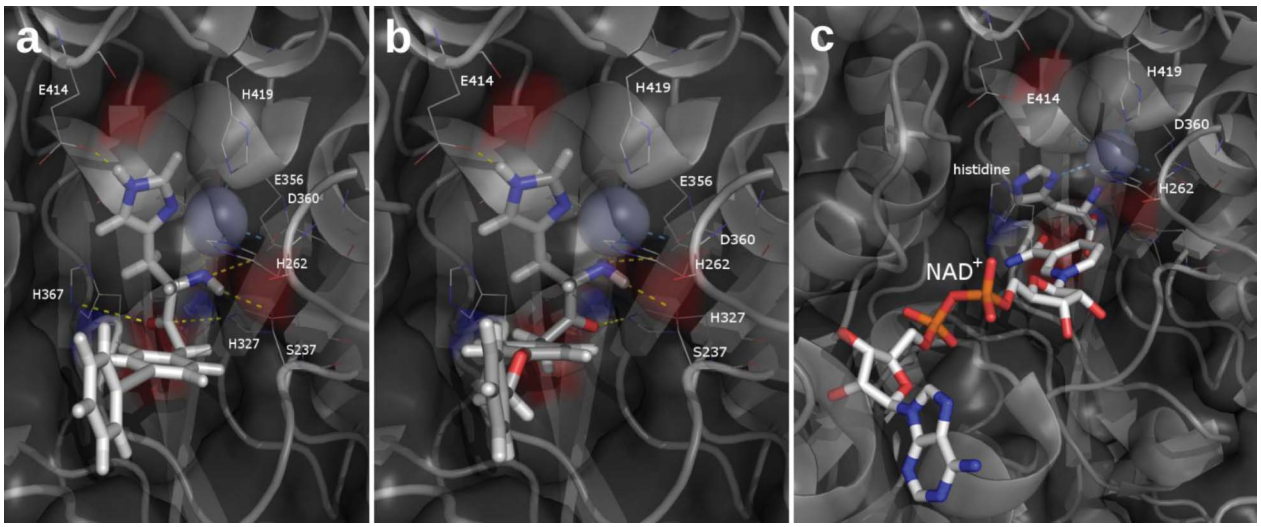

Fig. 5 Compound **7a** (a) compound **1** (b) and NAD^+/histidine co-crystallized (c) within the HDH enzymatic cavity; in yellow highlighted H-bonds stabilize the molecule (picture made with PYMOL)[11].

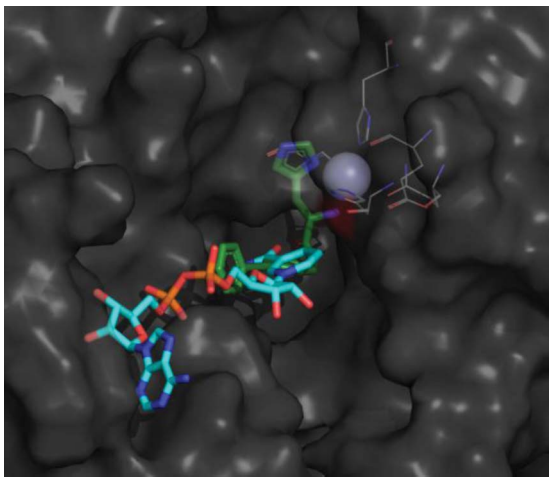

Fig. 6 Compounds **7a** and **NAD⁺** superimposed in the HDH enzymatic cavity (picture made with PYMOL).

Table 3 : Effect of the NAD^+ concentration on inhibition of *B. suis* HDH by inhibitor **7a**. The values are means of three independent assays. Variations were in the range of 5–10% of the shown data

NAD (mM)	Inhibitor (nM)	Conversion rate (ΔOD_{340}/5min)
2	0	0.51
2	3	0.22
10	3	0.48
10	15	0.16

Enzymatic assays: Competition between NAD^+ and HDH inhibitors

In order to confirm molecular modeling studies, the potential competition between NAD^+ and the HDH inhibitors in the enzymatic reaction was evaluated by varying NAD^+ concentrations in the measurement cell. Standard enzymatic kinetics were performed at a NAD^+ concentration of 2mM, being the optimal concentration of the cofactor for HDH activity (K_m = 12 μM). Influence of various NAD^+ concentrations on HDH inhibition measurement was evaluated, based on the previously established IC_{50} values of inhibitors (Table 3). In parallel, NAD^+ concentrations were maintained and inhibitor concentrations were modified. Obtained data show that NAD^+ concentration has a direct and proportional impact on IC_{50} values of the HDH inhibitor **7a**. The curves $1/V_i = f(1/C_i)$ revealed that V_{max} (0.0017 M s^{-1}) is not changing regardless of the inhibitor concentration used, whereas variation of the apparent K_m is observed (50-fold), confirming a competition between inhibitor and the cofactor NAD^+, and supporting the predicted orientation of the inhibitor structure in the lipophilic NAD^+-binding pocket.

Conclusions

By introduction of substituted aryl or substituted alkynyl aryl tails in the lead compound **1**, some potent and selective HDH inhibitors have been discovered.

Notable among these is compound **7a** with a phenyl alkynyl chain, possessing a strong inhibitory effect on HDH, with an IC_{50} of 3 nM. This compound was also able to impair growth of *B. suis in vitro* in minimal medium, and in the macrophage host cell. Molecular modeling and competition experiment with NAD^+ confirmed the positioning of the inhibitor inside the active site of HDH with an orientation of the imidazole ring in the hydrophilic histidine-binding pocket, and the other part of the structure oriented directly towards the second lipophilic NAD^+-binding pocket. As the target HDH has been directly linked to bacterial virulence, and with the results obtained on live extra- and intracellular brucellae, the development of these inhibitors can be considered as a promising step towards novel anti-virulence drugs.

Experimental Section

Chemistry

General. All reagents and solvents were of commercial quality and used without further purification, unless otherwise specified. All reactions were carried out under an inert nitrogen atmosphere. TLC analyses were performed on silica gel 60 F_{254} plates (Merck Art.1.05554). Spots were visualized under 254 nm UV illumination, or by ninhydrin solution spraying. Melting points were determined on a Büchi Melting Point 510 and are uncorrected. ^1H and ^{13}C NMR spectra were recorded on Bruker DRX-400 spectrometer using DMSO-d_6 as solvent and tetramethylsilane as internal standard. For ^1H NMR spectra, chemical shifts are expressed in δ (ppm) downfield from tetramethylsilane, and coupling constants (J) are expressed in Hertz. Electron Ionization mass spectra were recorded in positive or negative mode on a Water MicroMass ZQ.

Preparation of *tert*-butyl[(1*S*)-3-(4-bromophenyl)-1-({1-[(4-methoxyphenyl)(diphenyl)methyl]-1*H*-imidazol-4-yl}methyl)-2-oxopropyl]carbamate (2). A solution of the 4-bromophenylacetic acid (3 equiv.) in dry tetrahydrofuran (10 mL) was cooled to −78 °C and a solution of lithium bis(trimethylsilyl) amide (6 equiv., 1.06 M in tetrahydrofuran) was added dropwise. After 10 min, a solution of the protected histidine methyl ester (previously described in ref. 6) (1 equiv.) in tetrahydrofuran was introduced through a canula. The reaction was stirred for 16 h under argon allowing the mixture to warm to room temperature. The mixture was then extracted with ethyl acetate (100 ml) and washed with water (4 × 25 ml). The organic layer was dried over anhydrous magnesium sulfate and the solvent evaporated under reduced pressure to give yellowish viscous crude. The residue was purified by column chromatography on silica gel (CH_2Cl_2/Hexane/Acetone: 5/4/1) to give the fully protected final product as a white powder. ^1H NMR (DMSO- d_6, 400 MHz) 7.21 (m, 19H), 6.69 (s, 1H), 4.30 (m, 1H), 3.77 (s, 2H), 3.76 (s, 3H), 2.84 (dd, J = 6.0 Hz, 2H), 1.34 (s, 9H); ^{13}C (DMSO- d_6, 101 MHz) 206.4, 158.5, 155.2, 142.5, 137.7, 136.3, 134.1, 134, 131.9, 130.9, 130.6, 129.0, 128.0, 127.8, 119.6,119.1, 113.2, 78.3, 73.9, 55.0, 44.1, 28.4, 28.0; MS ESI⁺ m/z 682 $(M+H)^+$, 704 $(M+Na)^+$.

General procedure of the Suzuki cross coupling of compound 2 with various boronic acids. A 50 ml, two-necked round bottomed flask equipped with a magnetic stirring bar and a reflux condenser was charged with (1 eq) of compound **2** and 5 mL of toluene under argon atmosphere. The corresponding boronic acid (3 eq) was dissolved in a minimal amount of ethanol, and then transferred to the previous solution. The catalyst $Pd(PPh_3)_4$ (0.1 eq) was then

added, followed by (10 eq) of an aqueous solution of Na_2CO_3 (1 M). The resulting mixture was stirred for twelve hours under reflux. The reaction was monitored by mass spectroscopy. Upon completion, the mixture was extracted with ethyl acetate (50 ml) and washed with water (3 × 15 ml). The organic layer was dried over anhydrous magnesium sulfate and the solvent evaporated under reduced pressure to give yellowish viscous crude. The residue was purified by column chromatography on silica gel (CH_2Cl_2/Hexane/Acetone: 5/4/1) to give the fully protected final product, a white powder. This latter was deprotected under acidic conditions in a solution of HCl (4 M in dioxane), the reaction was monitored by TLC until all the starting material was consumed. The final dichlorohydrate salt was filtrated and washed with ether.

(3*S*)-3-Amino-4-(1*H*-imidazol-4-yl)-1-(4′-methylbiphenyl-4-yl)-butan-2-one dihydrochlorhydrate (3a). Mp 203 °C (decomposition); ^{1}H NMR (DMSO- d_6, 400 MHz) 9.13 (d, J = 1.1 Hz, 1H), 8.65 (s, 3H, NH_3^+), 7.57 (dd, J = 8.2 Hz, J = 17.6 Hz, 4H), 7.52 (s, 1H), 7.29 (dd, J = 8.1 Hz, J = 21.8 Hz, 4H), 4.73 (dd, J = 4.1 Hz, J = 7.9 Hz, 1H), 4.20 (s, 2H), 3.61 (dd, J = 4.4 Hz, J = 15.6 Hz, 1H), 3.24 (dd, J = 8.9 Hz, J = 15.5 Hz, 1H), 2.33 (s, 3H); ^{13}C (DMSO- d_6, 101 MHz) 202.8, 138.6, 136.9, 136.6, 134.1, 132.2, 130.4, 129.4, 126.5, 126.3, 126.2, 118.7, 56.9, 44.9, 24.2, 20.6; MS (ESI$^+$/ESI$^-$) m/z 320 (M+H)$^+$, 639 (2M+H)$^+$, 318 (M-H)$^-$, 354 (M+Cl)$^-$, 673 (2M+Cl)$^-$; Anal. Calcd for $C_{20}H_{23}Cl_2N_3O$: C, 61.23; H, 5.91; N, 10.71. Found: C, 61.27; H, 5.89; N, 10.74.

(3*S*)-3-Amino-1-(4′-butylbiphenyl-4-yl)-4-(1*H*-imidazol-4-yl)-butan-2-one dihydrochlorhydrate (3b). Mp 155 °C (decomposition); ^{1}H NMR (DMSO- d_6, 400 MHz) 9.13 (d, J = 1.3 Hz, 1H), 8.62 (m, 3H), 7.58 (dd, J = 8.3 Hz, J = 14.9 Hz, 4H), 7.52 (d, J = 0.9 Hz, 1H), 7.30 (dd, J = 8.3 Hz, J = 18.1 Hz, 4H), 4.73 (dd, J = 4.3 Hz, J = 9.0 Hz, 1H), 4.19 (s, 2H), 3.61 (dd, J = 4.4 Hz, J = 15.4 Hz, 1H), 3.23 (dd, J = 8.9 Hz, J = 15.5 Hz, 1H), 2.61 (t, J = 7.74 Hz, 2H), 1.57 (td, J = 7.5 Hz, J = 15.2 Hz, 2H), 1.32 (qd, J = 7.3 Hz, J = 14.5 Hz, 2H), 0.90 (t, J = 7.3 Hz, 3H); ^{13}C (DMSO- d_6, 101 MHz) 202.8, 141.5, 138.6, 137.1, 134.2, 132.2, 130.4, 128.8, 126.5, 126.3, 126.3, 118.3, 56.9, 44.9, 34.3, 33.0, 24.2, 21.7, 13.7; MS (ESI$^+$/ESI$^-$) m/z 362 (M+H)$^+$,723 (2M+H)$^+$,360 (M-H)$^-$, 396 (M+Cl)$^-$, 757 (2M+Cl)$^-$; Anal. Calcd for $C_{23}H_{29}Cl_2N_3O$: C, 63.59; H, 6.73; N, 9.67. Found: C, 63.56; H, 6.78; N, 9.63.

(3*S*)-3-Amino-4-(1*H*-imidazol-4-yl)-1-(4′-methoxybiphenyl-4-yl)butan-2-one dihydrochlorhydrate (3c). Mp 210 °C (decomposition); ^{1}H NMR (DMSO- d_6, 400 MHz) 14.82 (s, 2H), 9.13 (d, J = 1.1 Hz, 1H), 8.66 (s, 3H), 7.58 (dd, J = 8.6 Hz, J = 11.4 Hz, 4H), 7.52 (s, 1H), 7.30 (d, J = 8.3 Hz, 2H), 7.01 (d, J = 8.9 Hz, 2H), 4.73 (dd, 1H, J = 4.4 Hz, J = 8.6 Hz), 4.19 (s, 2H), 3.79 (s, 3H), 3.61 (dd, J = 4.3 Hz, J = 15.5 Hz, 1H), 3.25 (dd, J = 8.9 Hz, J = 15.4 Hz, 1H); ^{13}C (DMSO- d_6, 101 MHz) 202.9, 158.8, 138.3, 134.1, 132.1, 131.8, 130.4, 127.6, 126.5, 125.9, 118.2, 114.3, 56.9, 55.1, 44.9, 24.1; MS (ESI$^+$/ESI$^-$) m/z 336 (M+H)$^+$, 671 (2M+H)$^+$,334 (M-H)$^-$, 370 (M+Cl)$^-$, 705 (2M+Cl)$^-$; Anal. Calcd for $C_{20}H_{23}Cl_2N_3O_2$: C, 58.83; H, 5.68; N, 10.29. Found: C, 58.90; H, 5.5.62; N, 10.34.

(3*S*)-3-Amino-4-(1*H*-imidazol-4-yl)-1-[4′-(trifluoromethyl) biphenyl-4-yl] butan-2-one dihydrochlorhydrate (3d). Mp. 149 °C (decomposition); ^{1}H NMR (DMSO- d_6, 400 MHz) 14.78 (s, 2H), 9.12 (d, J = 1.3 Hz, 1H), 8.64 (s, 3H), 7.90 (d, J = 8.2 Hz, 2H), 7.81 (d, J = 8.3 Hz, 2H), 7.71 (d, J = 8.4 Hz, 2H), 7.52 (d, J = 1.1 Hz, 1H), 7.39 (d, J = 8.4 Hz, 2H), 4.75 (dd, J = 4.6 Hz, J = 8.9 Hz, 1H), 4.24 (s, 2H), 3.61 (dd, J = 4.3 Hz, J = 15.5 Hz, 1H), 3.24 (dd, J = 8.9 Hz, J = 15.5 Hz, 1H); ^{13}C (DMSO- d_6, 101 MHz) 202.7, 143.8, 137.0, 134.2, 133.8, 130.6, 127.8, 127.3, 126.8, 126.6, 125.7 (dd, $J_{C\text{-}F}$ = 3.6 Hz, $J_{C\text{-}F}$ = 7.3 Hz), 122.9, 118.2, 56.9, 44.9, 24.2; MS (ESI$^+$/ESI$^-$) m/z 374 (M+H)$^+$, 747 (2M+H)$^+$, 372 (M-H)$^-$, 408 (M+Cl)$^-$, 781 (2M+Cl)$^-$; Anal. Calcd for $C_{20}H_{20}Cl_2F_3N_3O$: C, 53.82; H, 4.52; N, 9.42. Found: C, 53.78; H, 4.45; N, 9.33.

(3*S*)-3-Amino-1-(4′-bromobiphenyl-4-yl)-4-(1*H*-imidazol-4-yl)-butan-2-one dihydrochlorhydrate (3e). Mp. 199 °C (decomposition); ^{1}H NMR (DMSO- d_6, 400 MHz) 14.51 (s, 2H), 9.11 (d, J = 1.0 Hz, 1H), 8.59 (s, 3H), 7.46 (m, 9H), 4.70 (dd, J = 4.2 Hz, J = 9.1 Hz, 1H), 4.14 (s, 2H), 3.58 (dd, 1H, J = 15.47, 4.33 Hz), 3.20 (dd, J = 9.0 Hz, J = 15.4 Hz, 1H); ^{13}C (DMSO- d_6, 101 MHz) 202.8, 134.2, 133.3, 130.4, 129.8, 128.9, 128.9, 128.2, 127.1, 126.8, 126.5, 118.2, 56.9, 45.2, 24.2; MS (ESI$^+$/ESI$^-$) m/z 383 (M+H)$^+$, 382 (M-H)$^-$, 416 (M+Cl)$^-$; Anal. Calcd for $C_{19}H_{20}BrCl_2N_3O$: C, 49.91; H, 4.41; N, 9.19. Found: C, 49.93; H, 4.35; N, 9.22.

(3*S*)-3-Amino-4-(1*H*-imidazol-4-yl)-1-(4′-phenoxybiphenyl-4-yl)butan-2-one dihydrochlorhydrate (3f). Mp 198–200 °C; ^{1}H NMR (DMSO- d_6, 400 MHz) 14.81 (s, 2H), 9.12 (d, J = 1.08 Hz, 1H), 8.66 (s, 3H), 7.68 (d, J = 8.76 Hz, 2H), 7.61 (d, J = 8.26 Hz, 2H), 7.52 (s, 1H), 7.42 (dd, J = 8.53, 7.47 Hz, 2H), 7.33 (d, J = 8.26 Hz, 2H), 7.17 (t, J = 7.39, 7.39 Hz, 1H), 7.11–7.04 (m, 4H), 4.74 (dd, J = 8.70, 4.53 Hz, 1H), 4.20 (s, 2H), 3.61 (dd, J = 15.46, 4.36 Hz, 1H), 3.24 (dd, J = 15.48, 8.86 Hz, 1H); ^{13}C (DMSO- d_6, 101 MHz) 202.8, 156.4, 156.3, 137.9, 134.9, 134.1, 132.3, 130.4–128.1, 126.6, 126.2, 123.6, 118.8, 118.2, 56.9, 44.9, 24.2; MS (ESI$^+$/ESI$^-$) m/z 398 (M+H)$^+$, 795 (2M+H)$^+$, 396 (M-H)$^-$, 432 (M+Cl)$^-$, 829 (2M+Cl)$^-$; Anal. Calcd for $C_{25}H_{25}Cl_2N_3O_2$: C, 63.83; H, 5.36; N, 8.93. Found: C, 63.88; H, 5.31; N, 8.91.

(3*S*)-3-Amino-4-(1*H*-imidazol-4-yl)-1-(1,1′:4′,1″-terphenyl-4-yl)butan-2-one dihydrochlorhydrate (3g). Mp 200 °C (decomposition); ^{1}H NMR (DMSO- d_6, 400 MHz) 14.71 (s, 2H), 9.12 (d, J = 1.18 Hz, 1H), 8.64 (s, 3H), 7.77 (m, 4H), 7.75–7.65 (m, 4H), 7.52 (s, 1H), 7.51–7.45 (m, 2H), 7.43–7.32 (m, 3H), 4.75 (dd, J = 8.70, 4.48 Hz, 1H), 4.22 (s, 2H), 3.62 (dd, J = 15.47, 4.33 Hz, 1H), 3.24 (dd, J = 15.52, 8.89 Hz, 1H); ^{13}C (DMSO- d_6, 101 MHz) 202.8, 139.5, 139.0, 138.7, 138.1, 134.2, 132.7, 130.5, 128.9, 127.5, 127.1, 127.0, 126.6, 126.5, 126.4, 118.3, 56.9, 44.9, 24.2; MS (ESI$^+$/ESI$^-$) m/z 382 (M+H)$^+$, 763 (2M+H)$^+$, 380 (M-H)$^-$, 416 (M+Cl)$^-$, 797 (2M+Cl)$^-$; Anal. Calcd for $C_{29}H_{27}Cl_2N_3O$: C, 69.05; H, 5.39; N, 8.33. Found: C, 69.11; H, 5.32; N, 8.28.

(3*S*)-3-Amino-4-(1*H*-imidazol-4-yl)-1-[4-(2-naphthyl)phenyl] butan-2-one dihydrochlorhydrate (3h). Mp 205 °C (decomposition); ^{1}H NMR (DMSO- d_6, 400 MHz) 14.86 (s, 2H), 9.14 (s, 1H), 8.69 (s, 3H), 8.22 (s, 1H), 8.00 (m, 2H), 7.94 (m, 1H),7.85 (dd, J = 1.6 Hz, J = 8.6 Hz, 1H), 7.79 (d, J = 8.2 Hz, 2H),7.53 (m, 3H), 7.40 (d, J = 8.2 Hz, 2H), 4.76 (dd, J = 4.7 Hz, J = 8.7 Hz, 1H), 4.25 (s, 2H), 3.63 (dd, J = 4.2 Hz, J = 15.4 Hz, 1H), 3.27 (dd, J = 9.1 Hz, J = 15.6 Hz, 1H); ^{13}C (DMSO- d_6, 101 MHz) 202.8, 138.4, 137.1, 134.1, 133.3, 132.8, 132.1, 130.5, 128.4–127.4, 126.8, 126.6–126.0, 125.0–124.9, 118.3, 56.9, 44.9, 24.2; MS (ESI$^+$/ESI$^-$) m/z 356 (M+H)$^+$, 713 (2M+H)$^+$; 354 (M-H)$^-$, 390 (M+Cl)$^-$, 745 (2M+Cl)$^-$; Anal. Calcd for $C_{29}H_{27}Cl_2N_3O$: C, 69.05; H, 5.39; N, 8.33. Found: C, 69.11; H, 5.38; N, 8.30.

(3*S*)-3-Amino-4-(1*H*-imidazol-4-yl)-1-[4-(2-phenylethyl) phenyl]butan-2-one dihydrochlorhydrate (4). Mp 168–170 °C; ^{1}H NMR (DMSO- d_6, 400 MHz) 9.11 (s, 1H), 8.63 (s, 3H), 7.50 (s, 1H), 7.31–7.20 (m, 4H), 7.21–7.08 (m, 5H), 4.69 (dd, J = 8.03, 4.09 Hz, 1H), 4.10 (s, 2H), 3.57 (dd, J = 15.41, 4.14 Hz, 1H), 3.21 (dd, J = 15.39, 8.89 Hz, 1H), 2.86 (s, 4H); ^{13}C (DMSO- d_6, 101 MHz) 202.9, 141.4, 140.0, 134.1, 130.7, 129.7–128.1, 126.5, 125.7, 118.2, 56.9, 44.9, 36.9, 36.6, 24.1; MS (ESI$^+$/ESI$^-$) m/z 334 (M+H)$^+$,667 (2M+H)$^+$, 332 (M-H)$^-$, 368 (M+Cl)$^-$, 701 (2M+Cl)$^-$; Anal. Calcd for $C_{21}H_{25}Cl_2N_3O$: C, 62.07; H, 6.20; N, 10.34. Found: C, 62.09; H, 6.25; N, 10.31.

(3*S*)-3-Amino-4-(1*H*-imidazol-4-yl)-1-{4-[(1*E*)-3-phenylprop-1-en-1-yl]phenyl}butan-2-one dihydrochlorhydrate (5). Mp 178–180 °C; ^{1}H NMR (DMSO- d_6, 400 MHz) 14.71 (s, 2H), 9.11 (d, J = 1.2 Hz, 1H), 8.61 (s, 3H), 7.50 (s, 1H), 7.27 (m, 9H), 6.47 (d, 1H, J = 15.8 Hz), 6.41 (dd, 1H, J = 16.5 Hz,J = 6.1 Hz), 4.69 (dd, J = 4.8 Hz, J = 8.7 Hz, 1H), 4.12 (s, 2H), 3.57 (dd, J = 4.3 Hz, J = 15.6 Hz, 1H), 3.52 (d, J = 5.6 Hz, 2H), 3.21 (dd, J = 8.9 Hz, J = 15.4 Hz, 1H); ^{13}C (DMSO- d_6, 101 MHz) 202.8, 139.9, 135.6, 134.1, 132.1, 130.1, 130.0, 129.2, 128.4, 128.4, 126.5, 125.9, 125.8, 118.2, 56.9, 44.9, 38.5, 24.1; MS (ESI$^+$/ESI$^-$) m/z 346 (M+H)$^+$, 691 (2M+H)$^+$, 344 (M-H)$^-$, 380 (M+Cl)$^-$, 725 (2M+Cl)$^-$; Anal. Calcd for $C_{22}H_{25}Cl_2N_3O$: C, 63.16; H, 6.02; N, 10.04. Found: C, 63.11; H, 5.95; N, 10.06.

(3*S*)-3-Amino-4-(1*H*-imidazol-4-yl)-1-{4-[(*E*)-2-phenylvinyl] phenyl}butan-2-one dihydrochlorhydrate (6a). Mp 195 °C (decomposition); ^{1}H NMR (DMSO- d_6, 400 MHz) 14.58 (s, 2H), 9.12 (d, J = 1.4 Hz, 1H), 8.61 (s, 3H), 7.59 (m, 3H), 7.51 (d, J = 1.2 Hz, 1H), 7.27 (m, 8H), 4.72 (dd, J = 4.5 Hz, J = 8.6 Hz, 1H), 4.16 (s, 2H), 3.59 (dd, J = 4.1 Hz, J = 15.3 Hz, 1H), 3.22 (dd, J = 8.9 Hz, J = 15.5 Hz, 1H); ^{13}C (DMSO- d_6, 101 MHz) 202.8, 136.9, 135.6, 134.2, 132.7, 130.2, 128.6, 128.2, 127.9, 127.6, 126.5, 126.4, 126.3, 118.2, 56.9, 45.0, 24.2; MS (ESI$^+$/ESI$^-$) m/z 332 (M+H)$^+$, 663(2M+H)$^+$, 330 (M-H)$^-$, 366 (M+Cl)$^-$, 697 (2M+Cl)$^-$; Anal. Calcd for $C_{21}H_{23}Cl_2N_3O$: C, 62.38; H, 5.73; N, 10.39. Found: C, 62.41; H, 5.80; N, 10.36.

(3*S*)-3-Amino-4-(1*H*-imidazol-4-yl)-1-{4-[(*E*)-2-(4-methyl phenyl)vinyl]phenyl}butan-2-one dihydrochlorhydrate (6b). Mp 200 °C (decomposition); ^{1}H NMR (DMSO- d_6, 400 MHz) 14.56 (s, 2H), 9.12 (d, J = 1.3 Hz, 1H), 8.61 (s, 3H), 7.54 (d, J = 8.3 Hz, 2H), 7.51 (d, J = 0.8 Hz, 1H), 7.49 (d, J = 8.2 Hz, 2H), 7.24 (d, J = 8.3 Hz, 2H), 7.18 (m, 4H), 4.71 (dd, J = 4.5 Hz, J = 8.0 Hz, 1H), 4.15 (s, 2H), 3.59 (dd, J = 4.5 Hz, J = 15.5 Hz, 1H), 3.22 (dd, J = 9.0 Hz, J = 15.5 Hz, 1H), 2.30 (s, 3H); ^{13}C (DMSO- d_6, 101 MHz) 202.8, 136.9, 135.8, 134.2, 132.5, 130.2, 129.2, 128.1, 126.9, 126.5, 126.3, 126.2, 118.2, 56.9, 45.0, 24.2, 20.8; MS (ESI$^+$/ESI$^-$) m/z 346 (M+H)$^+$, 691 (2M+H)$^+$, 344 (M-H)$^-$, 380 (M+Cl)$^-$, 725 (2M+Cl)$^-$; Anal. Calcd for $C_{22}H_{25}Cl_2N_3O$: C, 63.16; H, 6.02; N, 10.04. Found: C, 63.18; H, 6.08; N, 10.01.

(3*S*)-3-Amino-4-(1*H*-imidazol-4-yl)-1-(4-{(*E*)-2-[4-(trifluoro methyl)phenyl]vinyl}phenyl) butan-2-one dihydrochlorhydrate (6c). Mp 186 °C (decomposition); ^{1}H NMR (DMSO- d_6, 400 MHz) 14.56 (s, 2H), 9.13 (s, 1H), 8.62 (s, 3H), 7.82 (d, J = 8.1 Hz, 2H), 7.72 (d, J = 8.6 Hz, 2H), 7.62 (d, J = 8.2 Hz, 2H), 7.52 (d, J = 0.6 Hz, 1H), 7.43 (d, J = 16.6 Hz, 1H), 7.35 (d, J = 16.4 Hz, 1H), 7.28 (d, J = 8.1 Hz, 2H), 4.72 (s 1H), 4.18 (s, 2H), 3.60 (dd, J = 4.6 Hz, J = 15.8 Hz, 1H), 3.22 (dd, J = 9.2 Hz, J = 15.5 Hz, 1H); ^{13}C (DMSO- d_6, 101 MHz) 202.7, 141.1, 135.1, 134.1, 133.4, 130.9, 130.2, 127.2, 126.9, 126.7, 126.6, 126.5, 125.5, 122.9, 118.2, 56.9, 45.0, 24.1; MS (ESI$^+$/ESI$^-$) m/z 399 (M+H)$^+$,799 (2M+H)$^+$, 398 (M-H)$^-$, 434 (M+Cl)$^-$, 833 (2M+Cl)$^-$; Anal. Calcd for $C_{22}H_{22}Cl_2F_3N_3O$: C, 55.94; H, 4.69; N, 8.90. Found: C, 55.98; H, 4.72; N, 8.92.

(3*S*)-3-Amino-1-{4-[(*E*)-2-biphenyl-4-ylvinyl]phenyl}-4-(1*H*-imidazol-4-yl)butan-2-one dihydrochlorhydrate (6d). Mp 200 °C (decomposition); ^{1}H NMR (DMSO- d_6, 400 MHz) 14.54 (s, 2H), 9.12 (d, J = 1.3 Hz, 1H), 8.59 (s, 3H), 7.70 (m, 6H), 7.60 (d, J = 8.4 Hz, 2H), 7.51 (d, J = 1.0 Hz, 1H), 7.47 (t, J = 7.6 Hz, 2H), 7.37 (t, J = 1.2 Hz, 1H), 7.31 (m, 2H), 7.27 (d, J = 8.3 Hz, 2H), 4.72 (dd, J = 4.3 Hz, J = 8.3 Hz, 1H), 4.17 (s, 2H), 3.59 (dd, J = 4.3 Hz, J = 15.3 Hz, 1H), 3.22 (dd, J = 8.9 Hz, J = 15.5 Hz, 1H); ^{13}C (DMSO- d_6, 101 MHz) 202.8, 139.6, 139.1, 136.2, 135.7, 134.3, 132.8, 130.3–126.4, 118.3, 56.9, 45.1, 24.3; MS (ESI$^+$/ESI$^-$) m/z 408 (M+H)$^+$, 815 (2M+H)$^+$, 406 (M-H)$^-$, 442 (M+Cl)$^-$, 849 (2M+Cl)$^-$; Anal. Calcd for $C_{27}H_{27}Cl_2N_3O$: C, 67.50; H, 5.66; N, 8.75. Found: C, 67.45; H, 5.69; N, 8.72.

General procedure of the Sonogashira cross coupling of compound 2 with various substituted alkynes:. A 50 ml, two-necked round bottomed flask equipped with a magnetic stirring bar a rubber septum and a reflux condenser was charged with (1 equiv.) of compound X and 10 ml of dry THF under argon atmosphere. The corresponding alkyne (2equiv.) was added dropwise to the stirred solution as well as (2 equiv.) of the ligand PPh_3. The catalyst $Pd(PPh_3)_4$ (0.1 equiv.) was then added followed by (0.2 equiv.) of the cocatalyst CuI and the triethylamine (3 equiv.). The resulting mixture was stirred for twelve hours under reflux and the reaction was monitored by mass spectroscopy. The reaction mixture was extracted with dichloromethane (50 ml) and washed with water (3 × 15 ml). The organic layer was dried over anhydrous magnesium sulfate and the solvent evaporated under reduced pressure to give yellowish viscous crude. The residue was purified by column chromatography on silica gel (toluene–ethyl acetate: 7/3) to give the fully protected final product, a yellowish powder. This latter was deprotected under acidic conditions in a solution of HCl (4 M in dioxane), the reaction was monitored by TLC until all the starting material was consumed. The final salt was filtrated and washed with ether.

(3*S*)-3-Amino-4-(1*H*-imidazol-4-yl)-1-[4-(phenylethynyl) phenyl]butan-2-one dihydrochlorhydrate (7a). Mp 194 °C (decomposition); ^{1}H NMR (DMSO- d_6, 400 MHz) 14.69 (s, 2H), 9.11 (d, J = 1.1 Hz, 1H), 8.63 (s, 3H), 7.53 (m, 5H), 7.43 (m, 2H), 7.27 (m, 2H), 4.72 (dd, J = 4.2 Hz, J = 8.5 Hz, 1H), 4.23 (s, 2H), 3.59 (dd, J = 4.4 Hz, J = 15.4 Hz, 1H), 3.23 (dd, J = 8.9 Hz, J = 15.8 Hz, 1H); ^{13}C (DMSO- d_6, 101 MHz) 202.5, 134.2, 134.2, 132.1, 131.3, 131.2, 130.3, 128.7, 126.5, 122.2, 120.7, 118.2, 89.2, 89.1, 56.9, 45.1, 24.1; MS (ESI$^+$/ESI$^-$) m/z 330 (M+H)$^+$, 659 (2M+H)$^+$, 328 (M-H)$^-$, 364 (M+Cl)$^-$, 693 (2M+Cl)$^-$; Anal. Calcd for $C_{21}H_{21}Cl_2N_3O$: C, 62.69; H, 5.26; N, 10.44. Found: C, 62.73; H, 5.30; N, 10.42.

(3*S*)-3-Amino-4-(1*H*-imidazol-4-yl)-1-{4-[(4-methylphenyl) ethynyl]phenyl}butan-2-one dihydrochlorhydrate (7b). Mp 181 °C (decomposition); ^{1}H NMR (DMSO- d_6, 400 MHz) 14.53 (s, 2H), 9.13 (s, 1H), 8.64 (s, 3H), 7.46 (m, 5H), 7.26 (d, 4H), 4.72 (s large, 1H), 4.22 (s, 2H), 3.59 (dd, J = 4.5 Hz, J = 15.4 Hz, 1H), 3.23 (dd, J = 8. 9 Hz, J = 15.7 Hz, 1H), 2.33 (s, 3H); ^{13}C (DMSO- d_6,

101 MHz) 202.6, 138.5, 134.1, 134.0, 131.2, 131.1, 130.3, 129.3, 126.5, 120.9, 119.2, 118.3, 89.4, 88.5, 56.9, 45.1, 24.1, 20.9; MS (ESI$^+$/ESI$^-$) *m/z* 344 (M+H)$^+$, 687 (2M+H)$^+$; 342 (M-H)$^-$, 378 (M+Cl)$^-$, 722 (2M+Cl)$^-$; Anal. Calcd for $C_{22}H_{23}Cl_2N_3O$: C, 63.47; H, 5.57; N, 10.09. Found: C, 63.42; H, 5.61; N, 10.11.

(3*S*)-3-Amino-1-{4-[(4-*tert*-butylphenyl)ethynyl]phenyl}-4-(1*H*-imidazol-4-yl)butan-2-one dihydrochlorhydrate (7c). Mp 197 °C (decomposition); ^{1}H NMR (DMSO- d_6, 400 MHz) 14.49 (s, 2H), 9.11 (d, J = 1.3 Hz, 1H), 8.59 (s, 3H), 7.48 (m, 7H), 7.29 (d, J = 8.4 Hz, 2H), 4.72 (dd, J = 5.0 Hz, J = 8.8 Hz, 1H), 4.21 (s, 2H), 3.58 (dd, J = 4.5 Hz, J = 15.5 Hz, 1H), 3.21 (dd, J = 8.9 Hz, J = 15.5 Hz, 1H), 1.29 (s, 9H); ^{13}C (DMSO- d_6, 101 MHz) 202.5, 151.5, 134.3, 134.0, 131.1, 131.0, 130.3, 126.5, 125.5, 120.9, 119.3, 118.3, 89.4, 88.6, 56.9, 45.1, 34.5, 30.8, 24.2; MS (ESI$^+$/ESI$^-$) *m/z* 386 (M+H)$^+$, 771 (2M+H)$^+$, 384 (M-H)$^-$, 420 (M+Cl)$^-$, 805 (2M+Cl)$^-$; Anal. Calcd for $C_{25}H_{29}Cl_2N_3O$: C, 65.50; H, 6.38; N, 9.17. Found: C, 65.55; H, 6.35; N, 9.21.

(3*S*)-3-Amino-4-(1*H*-imidazol-4-yl)-1-{4-[(4-pentylphenyl)-ethynyl]phenyl}butan-2-one dihydrochlorhydrate (7d). Mp 184 °C (decomposition); ^{1}H NMR (DMSO- d_6, 400 MHz) 14.55 (s, 2H), 9.12 (d, J = 1.3 Hz, 1H), 8.62 (s, 3H), 7.50 (m, 5H), 7.26 (m, 4H), 4.72 (dd, J = 4.3 Hz, J = 8.2 Hz, 1H), 4.22 (s, 2H), 3.59 (dd, J = 4.5 Hz, J = 15.5 Hz, 1H), 3.22 (dd, 1H, J = 9.0 Hz, J = 15.5 Hz), 2.59 (t, J = 7.5 Hz, 2H), 1.57 (td, J = 7.5 Hz, J = 14.9 Hz, 2H), 1.27 (m, 4H), 0.85 (t, J = 7.0 Hz, 3H); ^{13}C (DMSO- d_6, 101 MHz) 202.5, 143.3, 134.2, 134.0, 131.2, 131.1, 130.3, 128.6, 126.5, 120.9, 119.4, 118.3, 89.4, 88.5, 56.9, 45.1, 34.9, 30.759, 30.3, 24.1, 21.8, 13.8; MS (ESI$^+$/ESI$^-$) *m/z* 400 (M+H)$^+$,799 (2M+H)$^+$, 398 (M-H)$^-$,434 (M+Cl)$^-$, 833 (2M+Cl)$^-$; Anal. Calcd for $C_{26}H_{31}Cl_2N_3O$: C, 66.10; H, 6.61; N, 8.89. Found: C, 66.15; H, 6.68; N, 8.82.

(3*S*)-3-Amino-1-[4-(biphenyl-4-ylethynyl)phenyl]-4-(1*H*-imidazol-4-yl)butan-2-one dihydrochlorhydrate (7e). Mp 196 °C (decompositon); ^{1}H NMR (DMSO- d_6, 400 MHz) 14.56 (s, 2H), 9.12 (d, J = 1.3 Hz, 1H), 8.61 (s, 3H), 7.73 (m, 4H), 7.64 (m, 2H), 7.56 (m, 2H), 7.52 (d, J = 1.0 Hz, 1H), 7.49 (m, 2H), 7.40 (m, 1H), 7.31 (m, 2H), 4.73 (dd, J = 4.3 Hz, J = 8.3 Hz, 1H), 4.23 (s, 2H), 3.60 (dd, J = 4.3 Hz, J = 15.7 Hz, 1H), 3.22 (dd, J = 8.9 Hz, J = 15.6 Hz, 1H); ^{13}C (DMSO- d_6, 101 MHz) 202.5, 140.2, 139.0, 134.2, 134.2, 131.9, 131.2, 130.3,129.0, 127.9, 126.9, 126.6, 126.5, 121.2, 120.7, 118.3, 89.9, 89.2, 57.0, 45.1, 24.2; MS (ESI$^+$/ESI$^-$) *m/z* 406 (M+H)$^+$, 811 (2M+H)$^+$, 404 (M-H)$^-$, 440 (M+Cl)$^-$,845 (2M+Cl)$^-$; Anal. Calcd for $C_{27}H_{25}Cl_2N_3O$: C, 67.78; H, 5.27; N, 8.78. Found: C, 67.72; H, 5.31; N, 8.72.

Enzyme assays

Cloning, overexpression of the HDH-encoding gene from *B. suis*, and purification of the enzyme were performed as previously described by our group.[6] The activity and specificity of HDH were measured by monitoring the reduction of NAD^+ to NADH directly at 340 nM (ε_M = 6200 M^{-1} cm^{-1}) as previously described.[12] The enzymatic activity was studied at 30 °C in the presence of 0.5 mM histidinol, 5 mM NAD^+ and 0.5 mM $MnCl_2$ in 50 mM sodium glycine buffer at pH 9.2. For kinetic studies, experiments were carried out with 150 mM sodium glycine (pH 9.2) and 2 mM NAD^+. The K_m for the substrate was determined by varying the concentration of histidinol from 10 to 50 µM and was found to be 12 µM. Activity (1 U) is defined as the amount of HDH producing 1 µmol of NADH per min in the reaction. To perform IC_{50} determinations of the different inhibitors, the latter were added at various concentrations, ranging from 1 to 200 nM, and preincubated for 5 min at 30 °C with the enzyme solution prior to the initiation of the reaction. The enzyme concentration in the assay system was 4.5 10^{-8} M.

Bacteriology and infection

***Brucella* culture in minimal medium in the presence of HDH inhibitors.** *B. suis* was grown in Gerhardt's minimal medium[13] at 37 °C to an optical density ($OD_{600\,nm}$) of 0.7. The culture was then diluted 1 : 100 in fresh minimal medium in the absence or presence of HDH inhibitor **7a** at 50 µM, respectively. Bacterial growth at 37 °C and under shaking was followed over a period of 7 days by $OD_{600\,nm}$ measurements.

Macrophage infection by *Brucella* in the presence of HDH inhibitors. Experiments were performed as described previously.[14] Briefly, differentiated human THP-1 macrophage-like cells were infected with early-stationary-phase *B. suis* for 45 min at a multiplicity of infection (MOI) of 20 bacteria per cell. Cells were washed twice with PBS and reincubated in RPMI 1640 with 10% fetal calf serum and gentamicin at 30 µg mL^{-1} for at least 1 h at 37 °C and 5% CO_2 to kill extracellular bacteria. At 90 min. post infection, cells of the appropriate culture wells were washed twice with PBS and lysed in 0.2% Triton X-100. The number of intracellular living bacteria was determined by plating serial dilutions on TS agar plates and incubation at 37 °C for 3 days. Half of the wells infected for lyses points and enumeration at 4, 7, and 24 h were then incubated in fresh medium in the presence of the HDH inhibitor **7a** at concentrations of 5 or 10 µM, respectively, the other half of the wells contained only fresh RPMI 1640 with 10% fetal calf serum and gentamicin at 30 µg ml^{-1}. Experiments were performed three times in triplicate.

Acknowledgements

This work was supported by a grant from the German Sanitätsamt der Bundeswehr, No. M SAB1 5A002, and by ANR grant ANR-09-MIEN-001 (to SK and J-Y W).

J.M. would like to thanks Dr Raphael Frederick for very fruitful discussions and Pr Johan Wouters for providing access to his molecular modeling platform.

References

1 D. J. Payne, M. N. Gwynn, D. J. Holmes and D. L. Pompliano, Drugs for bad bugs: confronting the challenges of antibacterial discovery., *Nat. Rev. Drug Discovery*, 2006, **6**, 29–40.

2 (*a*) S. Escaich, Antivirulence as a new antibacterial approach for chemotherapy., *Curr. Opin. Chem. Biol.*, 2008, **12**, 400–408; (*b*) L. Cegelski, G. R. Marshall, G. R. Eldridge and S. J. Hultgren, The biology and future prospects of antivirulence therapies., *Nat. Rev. Microbiol.*, 2008, **6**, 17–27; (*c*) D. A. Rasko and V. Sperandio, Anti-virulence strategies to combat bacteria-mediated disease., *Nat. Rev. Drug Discovery*, 2010, **9**, 117–128.

3 (*a*) S. Köhler, V. Foulongne, S. Ouahrani-Bettache, G. Bourg, J. Teyssier, M. Ramuz and J-P. Liautard, The analysis of the intramacrophagic virulome of *Brucella suis* deciphers the environment encountered by the pathogen inside the macrophage host cell., *Proc. Natl. Acad. Sci. U. S. A.*, 2002, **99**, 15711–15716; (*b*) S. Köhler, S. Michaux-Charachon, F. Porte, M. Ramuz and J-P. Liautard, What is the nature of the

replicative niche of a stealthy bug named Brucella?, *Trends Microbiol.*, 2003, **11**, 215–219.
4 (*a*) I. Lopes-Goni and I. Moriyon, *Brucella: Molecular and Cellular Biology*Horizon Bioscience, 2004: 1–432; (*b*) H. Guerra, The brucellae and their success as pathogens., *Crit. Rev. Microbiol.*, 2007, **33**, 325–331; (*c*) M. P. Franco, M. Mulder, R. H. Gilman and H. L. Smits, Human brucellosis., *Lancet Infect. Dis.*, 2007, **7**, 775–786; (*d*) G. Pappas, P. Papadimitriou, N. Akritidis, L. Christou and E. V. Tsianos, The new global map of human brucellosis., *Lancet Infect. Dis.*, 2006, **6**, 91–99.
5 (*a*) C. T. Supuran, J-Y. Winum, Introduction to zinc enzymes as drug targets. In *Drug Design of Zinc-Enzyme Inhibitors: Functional, Structural, and Disease Applications*, C. T. SupuranJ. Y. Winum ed., Wiley, Hoboken, 2009, pp. 3–12; (*b*) J-Y. Winum, S. Köhler, A. Scozzafava, J-L. Montero and C. T. Supuran, Targeting bacterial metalloenzymes: A new strategy for the development of anti-infective agents., *Anti-Infect. Agents Med. Chem.*, 2008, **7**, 169–179.
6 (*a*) M. R. Abdo, P. Joseph, R. A. Boigegrain, J-P. Liautard, J-L. Montero, S. Köhler and J-Y. Winum, *Brucella suis* histidinol dehydrogenase: synthesis and inhibition studies of a series of substituted benzylic ketones derived from histidine., *Bioorg. Med. Chem.*, 2007, **15**, 4427–4433; (*b*) P. Joseph, M. R. Abdo, R. A. Boigegrain, J-L. Montero, J-Y. Winum and S. Köhler, Targeting of the *Brucella suis* virulence factor histidinol dehydrogenase by histidinol analogues results in inhibition of intramacrophagic multiplication of the pathogen., *Antimicrob. Agents Chemother.*, 2007, **51**, 3752–3755; (*c*) M. R. Abdo, P. Joseph, R. A. Boigegrain, J-P. Montero, S. Köhler and J-Y. Winum, *Brucella suis* histidinol dehydrogenase: synthesis and inhibition studies of substituted N-L-histidinylphenylsulfonyl hydrazide., *J. Enzyme Inhib. Med. Chem.*, 2008, **23**, 357–361.
7 (*a*) P. I. Fields, R. V. Swanson, C. G. Haidaris and F. Heffron, Mutants of *Salmonella typhimurium* that cannot survive within the macrophage are avirulent., *Proc. Natl. Acad. Sci. U. S. A.*, 1986, **83**, 5189–5193; (*b*) S. Pilatz, K. Breitbach, N. Hein, B. Fehlhaber, J. Schulze, B. Brenneke, L. Eberl and I. Steinmetz, Identification of *Burkholderia pseudomallei* genes required for the intracellular life cycle and *in vivo* virulence., *Infect. Immun.*, 2006, **74**, 3576–3586; (*c*) T. Parish, Starvation survival response of *Mycobacterium tuberculosis*., *J. Bacteriol.*, 2003, **185**, 6702–6706.
8 S. F. Altschul, T. L. Madden, A. A. Schaffer, J. H. Zhang, Z. Zhang, W. Miller and D. J. Lipman, Gapped BLAST and PSI-BLAST: a new generation of protein database search programs., *Nucleic Acids Res.*, 1997, **25**, 3389–3402.
9 J. A. Barbosa, J. Sivaraman, Y. Li, R. Larocque, A. Matte, J. D. Schrag and M. Cygler, Mechanism of action and NAD+-binding mode revealed by the crystal structure of L-histidinol dehydrogenase., *Proc. Natl. Acad. Sci. U. S. A.*, 2002, **99**, 1859–1864.
10 G. Jones, P. Willett, R. C. Glen, A. R. Leach and R. Taylor, Development and validation of a genetic algorithm for flexible docking., *J. Mol. Biol.*, 1997, **267**, 727–748.
11 W. L. Delano, The PyMOL Molecular Graphics System on World Wide Web. http://pymol.sourceforge.net/(accessed June 21 2010).
12 J. C. Loper and E. Adams, Purification and Properties of Histidinol Dehydrogenase from *Salmonella typhimurium.*, *J. Biol. Chem.*, 1965, **240**, 788–795.
13 M. Dozot, R. A. Boigegrain, R. M. Delrue, R. Hallez, S. Ouahrani-Bettache, I. Danese, J. J. Letesson, X. De Bolle and S. Köhler, The stringent response mediator Rsh is required for *Brucella melitensis* and *Brucella suis* virulence, and for expression of the type IV secretion system virB., *Cell. Microbiol.*, 2006, **8**, 1791–1802.
14 S. Burkhardt, M. P. Jiménez de Bagüés, J-P. Liautard and S. Köhler, Analysis of the behavior of eryC mutants of *Brucella suis* attenuated in macrophages., *Infect. Immun.*, 2005, **73**, 6782–6790.

